Stochastic Resonance for Weak Signal Detection

Phase-II Project Report

Submitted by

S Harivignesh
(121901015)

under the guidance of

Dr. Arvind Ajoy

INDIAN INSTITUTE
OF TECHNOLOGY
PALAKKAD

DEPARTMENT OF ELECTRICAL ENGINEERING

CERTIFICATE

*This is to certify that the work contained in this thesis entitled "**Stochastic Resonance for Weak Signal Detection**" is a bonafide work of **S Harivignesh** (**Roll No. 121901015**), carried out in the Department of Electrical Engineering, Indian Institute of Technology Palakkad under my supervision and that it has not been submitted elsewhere for a degree.*

Dr. Arvind Ajoy

Associate Professor

Department of Electrical Engineering

Indian Institute of Technology Palakkad

Contents

List of Figures

List of Tables

Chapter 1

Introduction to Stochastic Resonance

Stochastic Resonance (SR) is a counterintuitive phenomenon where adding the right amount of noise to certain systems increases the Signal to Noise Ratio(SNR) at the output. The amount of noise applied is quantified by its variance, but this detail is ignored in discussions. Stochastic resonance(SR) is observed in two kinds of systems: threshold-based systems and double-well potential systems. In threshold-based systems, the effect of SR is observed because the noise directly helps the sub-threshold signal to cross the system's threshold at regular intervals, which is reflected in the output as a signal with a frequency component the same as that of the sub-threshold signal. While in double-well potential systems, for a sub-threshold input signal, the system is essentially transparent with minimal signal distortion and almost the same amplitude of the signal. White Gaussian Noise (WGN) applied to the input of a double-well potential system is reflected as a random walk process in the output, with the variance of its distribution increasing over time. This means that, given any arbitrary amount of noise, the output will eventually cross the potential barrier and switch to the other state. The matter of concern in these systems is to facilitate switching in a reasonable amount of time or within nearly a specific amount of time of interest. When the right amount of noise is added to the input, it helps the system's

output change from one state to the other at regular intervals. When the noise added facilitates the switching of the state within half the period of the driving sub-threshold signal, the corresponding frequency component in the output signal's spectrum is boosted. For a small amount of noise, the noise applied is not enough to facilitate the switching in a reasonable amount of time, and the Signal-to-Noise Ratio(SNR) of the output will be low since the signal is also not present or weakly present at the output. For high amounts of noise, the features of the sub-threshold signal will be lost and only noise will be observed at the output, and the SNR at the output will be low again. But for the right amount of noise applied, the output will have a significant representation of the applied sub-threshold signal, and the SNR will be high. This is the stochastic resonance phenomenon.

1.1 Organization of The Report

This chapter introduced the phenomenon of stochastic resonance. Chapter 2 discusses the prior works on this topic of stochastic resonance from OELP and BTP and also describes the double-well system in detail. Chapter 3 presents the frequency response analysis of the double-well system through different methods and proposes the necessary conditions on the sub-threshold signals and the noise to be able to observe stochastic resonance in general. Chapter 4 discusses the generation of noise using the function generators and the observations from the experiments. Chapter 5 discusses in detail how to use MATLAB to automate the test setup to generate data using the function generator and to acquire data using the oscilloscope. It also discusses some practical details on generating noise with constant variance. Chapter 6 discusses the practical system model for the hardware implementation and presents experimental data of the outputs. It also presents some results indicating the observation of stochastic resonance with a boosted SNR at the output for the right amount of noise. Finally, chapter 7 concludes and discusses future work. And references are included at the last.

Chapter 2

Review of Prior Works

In this chapter, we describe the system where stochastic resonance is studied. We also discuss the details of necessary quantities associated with the system under consideration which are necessary for the study of stochastic resonance. We also discuss the previous works so far in this study of stochastic resonance.

2.1 Description of the Double-well Potential System

Stochastic resonance is observed in the over-damped 1-D Brownian motion of a particle in a double-well potential system given in figure 2.1. The differential equation modeling this system is given by,

$$\frac{dx}{dt} = -\frac{dU(x)}{dx} + \eta(t) + Acos(\omega t) \tag{2.1}$$

$$U(x) = -\frac{ax^2}{2} + \frac{bx^4}{4} \tag{2.2}$$

where x is the position of the particle in 1-D space, $U(x)$ is the potential function, $\eta(t)$ is zero-mean white Gaussian noise with variance D whose autocorrelation is given by $<\eta(t)\eta(\tau+t)>= D\delta(t)$, and $Acos(\omega t)$ is the signal modulating the double-well system. The threshold for the modulating signal's amplitude A beyond which there is only one minimum

in the potential function as in figure 2.2b is given by,

$$A_t = \pm \frac{2a}{3}\sqrt{\frac{a}{3b}} \\ = \pm\, 0.3849 \cdot a\sqrt{\frac{a}{b}} \tag{2.3}$$

The particle is forced to the minima for A greater than A_t. The mean first passage time of the particle from one well to the other well is called Kramers time[1]. The expression of Kramers time[2] is given by

$$\tau_k = \frac{2\pi e^{2\Delta U/D}}{\left|\ddot{U}(x_{min})\ddot{U}(x_{max})\right|^{1/2}} \tag{2.4}$$

where ΔU is the potential difference between the maxima and one of the minima. x_{min} and x_{max} are the location of the minima and maxima respectively. In the absence of modulation $\Delta U = U_o$, $x_{min} = \pm 1$ and $x_{max} = 0$. The Kramers rate r_k is defined as the reciprocal of τ_k. The probability of finding the particle in a well decays exponentially with time[2] and the expression is given by

$$p(t) = e^{-r_k t} \tag{2.5}$$

The switching probability of the particle is the complement of $p(t)$ and is given by,

$$s(t) = 1 - e^{-r_k t} \tag{2.6}$$

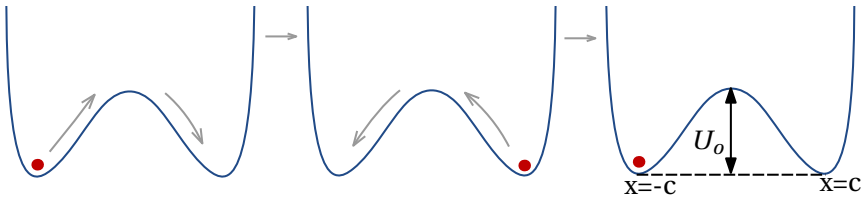

Fig. 2.1: Double-well system

2.2 OELP

The goal in OELP was to implement the circuit model for the over-damped 1D Brownian motion of a particle in a double-well potential[3] in LTspice and verify the behavior of this system's output. The circuit implementation of this system in LTspice is given in figure 2.3. The Kramers time statistic was used to verify the circuit implementation's behavior. The Kramers time is the average time spent by the particle in a well before switching to the other well of the double-well potential. The analytical expression for the Kramers time for this system[2, 3] was used to verify the results from the simulations. It was observed that when the bandwidth of the noise was changed, the output due to the noise attenuated leading to no switching events observed at the output. An analytical criterion based on the expression for the FFT of the noise at the output was proposed to ensure switching events at the output. Following this, based on the idea of combing the survival probability of the particle in one of the wells[4] with the random number generation in ferroelectrics[5] which has the same characteristics as the double-well system under consideration, we implemented a true random number generator in LTspice. It was followed by testing the randomness of the random numbers generated using the NIST statistical test suite. Periodic switching for a subthreshold signal in this system for a certain variance of noise as the input was also observed and this is the stochastic resonance phenomenon. Stochastic resonance based detection for a binary FSK signal[6] was also implemented towards the end of the OELP.

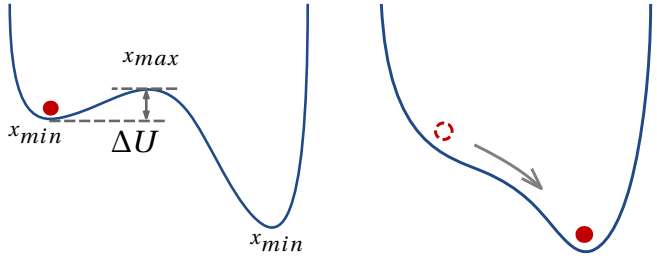

(a) Subthreshold biasing (b) Suprathreshold biasing

Fig. 2.2: Subthreshold and Suprathreshold modulations

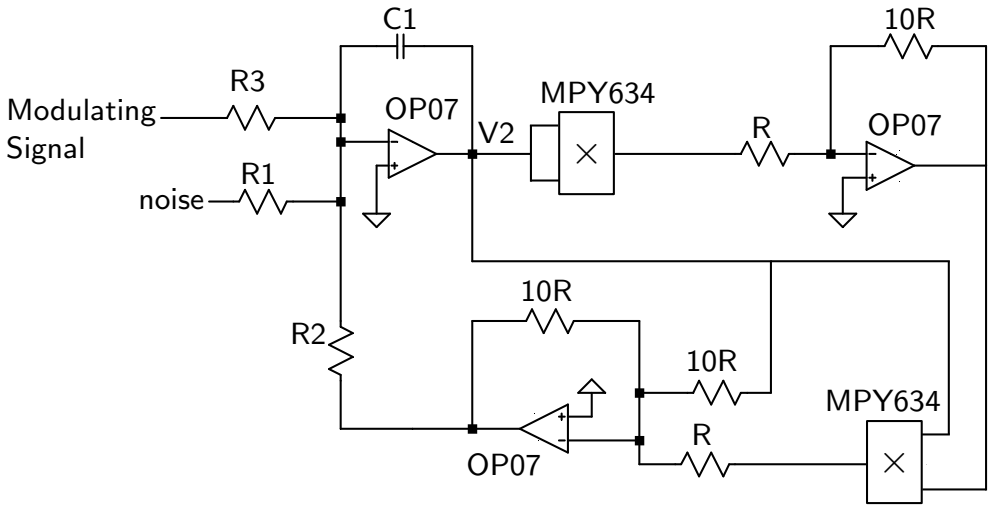

Fig. 2.3: LTspice implementation of the over-damped 1D Brownian motion of a particle in a double-well potential

2.3 BTP Phase I

The goal of the BTP was to implement the circuit model of LTspice and to observe stochastic resonance in the hardware. The circuit was wired up in a breadboard and the noise from the built-in noise mode of the function generator was given as the input. But there were no switching events observed at the output for any peak-to-peak voltage of noise. Hence to remove any uncertainties in the breadboard implementation, a PCB was designed. Following this, a literature review on the applications of stochastic resonance was presented towards the end of BTP Phase I.

2.4 BTP Phase II up to Midterm

The double-well potential is a characteristic of ferroelectrics' free energy vs polarization. Initially, the results from the literature on measuring the negative capacitance behavior of the double-well system in ferroelectrics were replicated in numerical simulation. To experiment with ferroelectrics for observing stochastic resonance, a ferroelectric thin film material made out of PVDF was fabricated and its characteristics were analyzed using X-ray diffraction and Scanning Electron Microscope instruments. It was found that the

PVDF material did not form a thin film, instead patches of PVDF material were formed. This could have been due to uneven annealing of the wafer and poor temperature control of the hot plate used for annealing. Following this we moved on to fabricate the PCB designed in the previous phase to try to observe stochastic resonance experimentally. The PCB was fabricated and populated and is given in figure 2.4. Deterministic switching of the output voltage for suprathreshold sinusoidal signal was observed towards the middle of the BTP phase II.

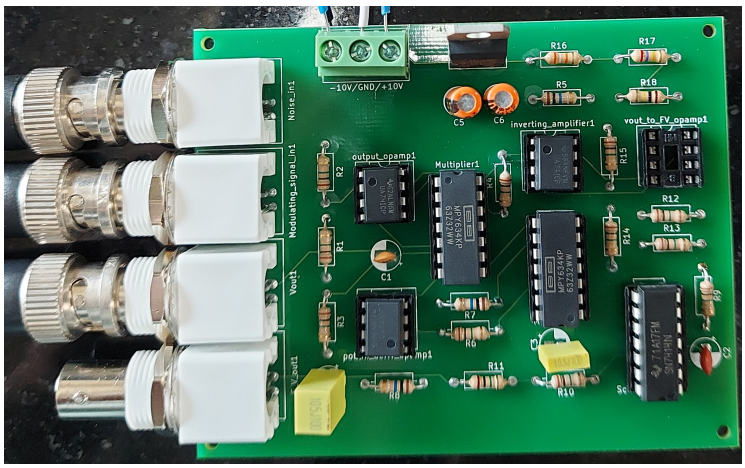

Fig. 2.4: The hardware implementation of the over-damped 1D Brownian motion of a particle in a double-well potential

2.5 Conclusion

This chapter describes the double-well potential system and lists important quantities describing the behavior of the system which are necessary for the analysis of stochastic resonance in the system. A review of the previous work on this topic of stochastic resonance starting from OELP and BTP Phase-I up to the middle of the BTP Phase-II.

Chapter 3

Frequency Response Analysis

In this chapter, the frequency response of the over-damped double-well potential system is studied. Since this is a non-linear system, it is not possible to find the frequency response analytically. Instead approximating the non-linear system with a linear system about an operating point and numerical methods are followed to find the frequency response and they are discussed in this chapter. Finding how the parameters in this system affect the frequency response will enable us to increase the operating frequency of the input signals and understand the bandwidth requirements of the noise input.

3.1 AC Analysis of the System in LTspice

The differential equation for the over-damped 1D Brownian motion in a double-well potential's circuit model in LTspice, given in figure 2.3, is given by,

$$\frac{\mathrm{d}V_2}{\mathrm{d}t} = -\frac{1}{C_1}\left(\frac{-V_2 + V_2^3}{R_2} + \frac{f(t)}{R_1} - \frac{A cos(\omega t)}{R_3}\right) \tag{3.1}$$

where $f(t)$ is the noise which is set to zero and instead of $Acos(\omega t)$ as the input, an independent voltage source with the small signal AC analysis amplitude as 1 is used for the AC analysis in LTspice.

The LTspice's AC analysis computes complex node voltages as a function of frequency. All nonlinear devices are approximated with a linearized model about a DC operating point. The resultant linearized circuit is used to find the frequency response of the circuit. The frequency response obtained from the LTspice's AC analysis for the over-damped double-well potential system's circuit model is given in figure 3.1. The obtained frequency response is having a low-pass filter response with a 20 dB/decade roll-off rate and a 3 dB bandwidth of approximately 1.5 kHz and unity gain as measured from the AC analysis. The op07 opamp is used in LTspice simulation and its unity gain bandwidth is approximately 757 kHz as measured in an AC analysis. Hence beyond 1 MHz the frequency response has a higher roll-ff rate and the analysis is considered for only up to 1 MHz.

It is observed that the bandwidth of the low-pass frequency response of this system is directly proportional to the coefficients of the double-well potential function which is $1/R_2C_1$ in the circuit model implemented in LTspice. The AC analysis is repeated for different values of capacitance C_1 and the frequency responses are given in figure 3.2. The approximate relation observed is

$$Bandwidth \approx \frac{1}{10R_2C_1} \tag{3.2}$$

3.2 Numerical Frequency Response Analysis

The differential equation of the over-damped double-well potential system used for the numerical simulation is given by,

$$\frac{dx}{dt} = ax - bx^3 + \eta(t) + Acos(\omega t) \tag{3.3}$$

where $\eta(t)$ is the noise and $Acos(\omega t)$ is the sinusoidal input to the system. Here variable x is equivalent to the voltage v2 in the circuit model.

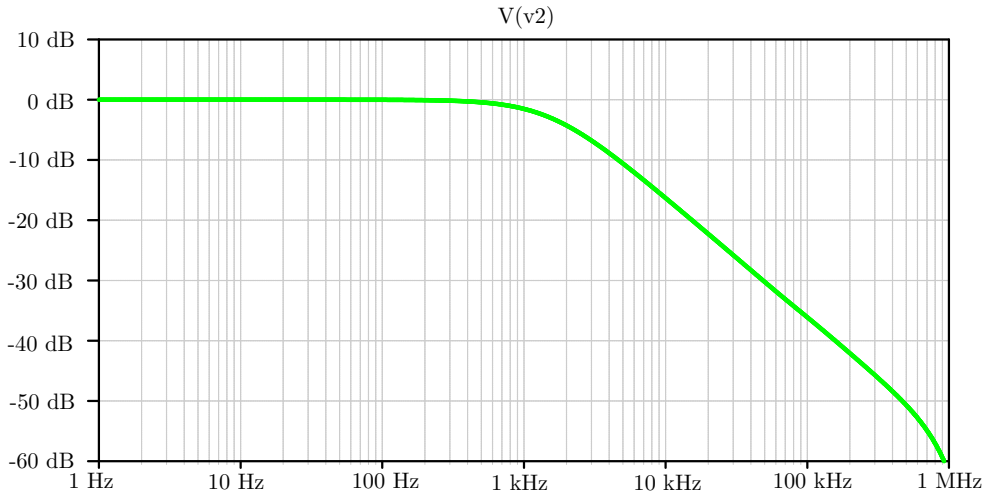

Fig. 3.1: Frequency response of over-damped double-well potential system's circuit model from LTspice AC analysis with the parameter $(1/R_2C_1) = 10^4\ Hz$.

The frequency response was estimated numerically for the individual harmonics by exciting the system with a sinusoid of a particular frequency and measuring the magnitude of the different harmonics of the fundamental frequency at the output[7]. The numerical simulation was performed for a discrete number of input sinusoids and later the output frequency response for individual harmonics was interpolated to get a continuous response. The resultant frequency response is given in figure 3.3. It is observed from the numerical simulations that the output has only odd harmonics with the fundamental frequency i.e., the first harmonic being the predominant one, while the higher-order harmonics are quite insignificant in magnitude compared to the first harmonic.

The numerical frequency response given in figure 3.4 is performed for the parameter values $a = b = 10^4$ which is the same as that of the frequency response of the LTspice AC analysis with $(1/R_2C_1) = 10^4$ Hz of figure 3.1. The first harmonic response from the numerical simulation has a low-pass response similar to the LTspice AC analysis and a 3 dB bandwidth of approximately 2 kHz. Similar to the LTspice AC analysis, from the numerical simulations, it is observed that the bandwidth is proportional to the coefficients

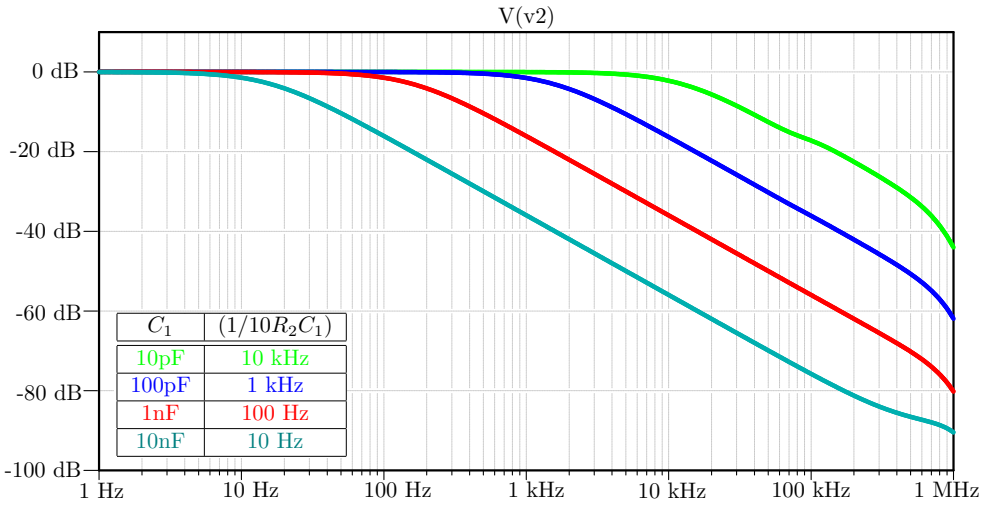

Fig. 3.2: Frequency response of over-damped double-well potential system's circuit model from LTspice AC analysis for different values of capacitance C_1.

a and b of the double-well function approximately given by,

$$Bandwidth \approx \frac{a}{5}; \quad with\ a = b. \tag{3.4}$$

3.3 Adomian Decomposition Method for Solving Non-linear Differential Equations in Approximation

Adomian Decomposition method[8] gives a series approximation for the solutions of non-linear differential equations in the time domain. It could be possible that the approximate frequency response of a non-linear system can be obtained via this method. The time domain series approximation of the solution could be obtained for a sinusoidal input to the system. From the Fourier transform of this series approximation, analytical expressions for the frequency response of the individual harmonics of all the frequencies could be obtained. This would give an analytical relation between the parameters of the system to the characteristics of the frequency response. In our problem, this could be the analytical expression for the relation between the bandwidth of the low-pass frequency response and the parameters of the non-linear system.

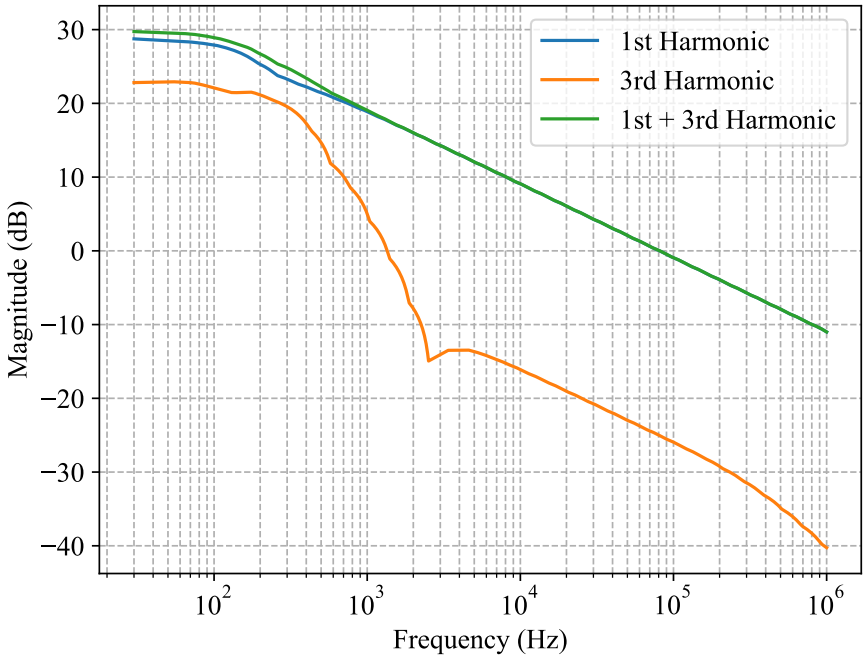

Fig. 3.3: Frequency response of over-damped double-well potential system's harmonics for sinusoidal inputs with $a = b = 10^3$

3.4 Inference from the Frequency Response Analysis

3.4.1 Frequency of the Weak Signal

This project aims to use stochastic resonance for weak signal detection. Increasing the frequency of the weak signals that can be detected using this method is also of interest to us. It is observed from frequency response analysis that our stochastic resonance system of interest, the over-damped double-well potential system, has a low-pass response. This limits the frequency of the weak signals that can be detected by this system to the bandwidth of the low-pass response. Any higher frequency weak signal that needs to be detected will get attenuated by the system. Hence the bandwidth of the system needs to be higher than the frequency of the weak signal that needs to be detected which can be achieved by changing the resistance and capacitance according to the equation 3.2.

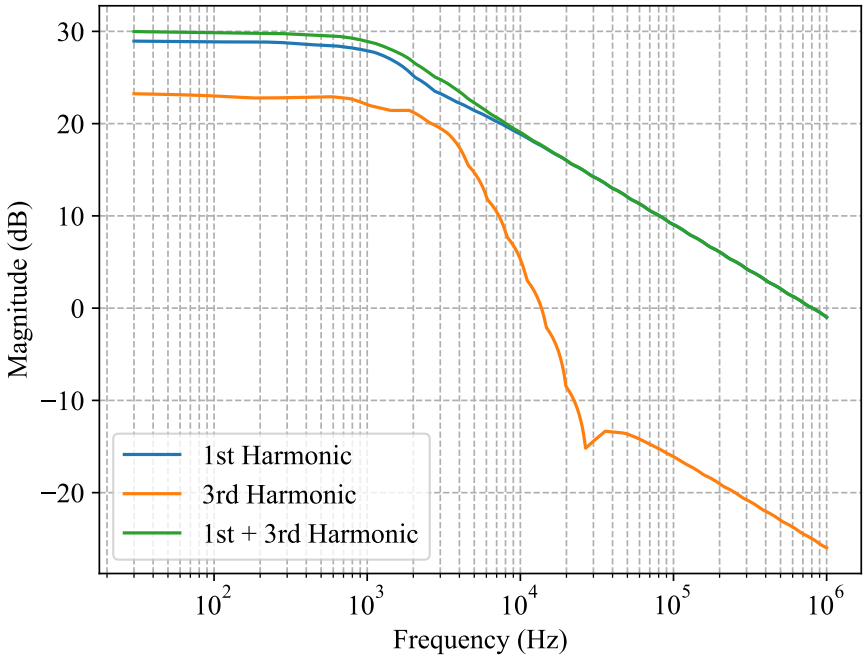

Fig. 3.4: Frequency response of over-damped double-well potential system's harmonics for sinusoidal inputs with $a = b = 10^4$

3.4.2 Bandwidth of the Noise

Practically, noise is characterized by it's variance (σ^2), bandwidth (B) and power spectral density (PSD) and their relation is given by,

$$PSD = \frac{Variance}{Bandwidth} = \frac{\sigma^2}{B} \tag{3.5}$$

The variance of noise is the power delivered by the noise which is the product of its PSD and bandwidth. When the bandwidth reduces because of the filtering of the noise, the bandwidth decreases while the PSD remains constant. Hence the power i.e., the variance of the noise decreases. This is depicted in figure 3.5 where noise is generated with a particular bandwidth and variance in MATLAB and is filtered with a unity gain low-pass filter. The resultant noise has a lower variance because of reduced bandwidth but a constant power spectral density. The variance of the noise is critical for stochastic resonance. Hence

for observing stochastic resonance, for a given noise variance, the bandwidth of the noise given as input should be less than the bandwidth of the low-pass response of the over-damped double-well potential system. The requirements on the bandwidth of the noise

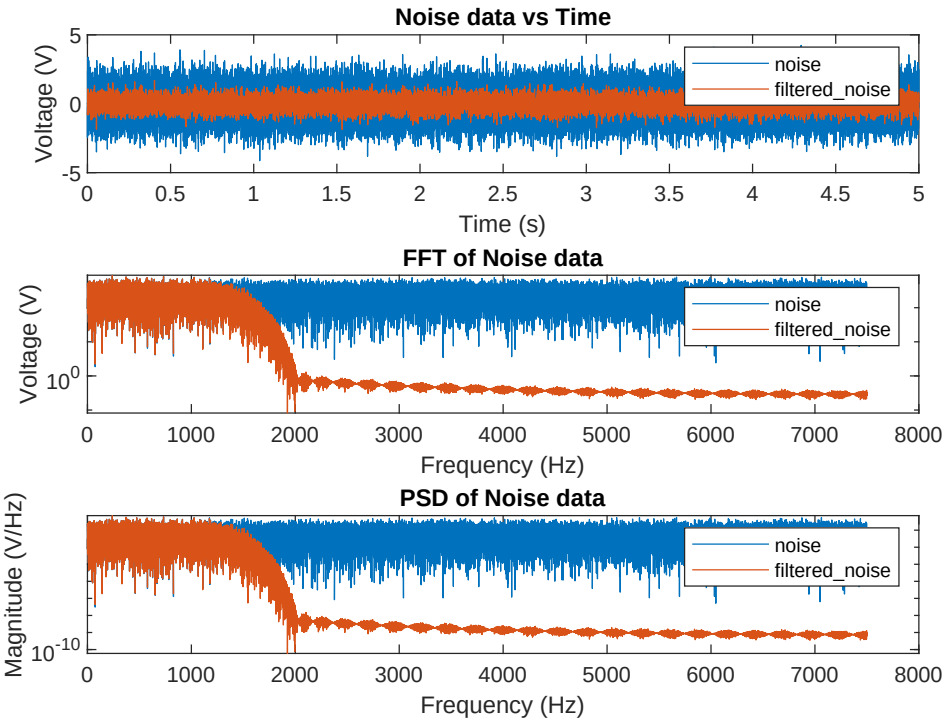

Fig. 3.5: Noise data before and after lowpass filtering

for observing stochastic resonance for a weak signal of a certain frequency still need to be studied. Intuitively, the bandwidth of the noise needs to be at least greater than the frequency of the weak signal, for the noise to enable switching within one half cycle of the weak signal. If the bandwidth of the noise is quite low, then the applied noise may have a constant amplitude over the period of the weak signal which will defeat the purpose of applying noise in the first place. Because the applied white Gaussian noise gets integrated into a random walk process at the output whose variance increases with time that causes the output to switch to the other minima of the double-well potential within the half cycle of the weak signal. And this process will not happen if the applied noise is constant over the period of the weak signal. From the experiments, it is observed that the higher the

bandwidth of the noise and the bandwidth of the stochastic resonance system compared to that of the weak signal's frequency, the better the output's switching profile in terms of the steepness of the output when it switches to the other minima and in the consistency of the time that the output stays in one of the minima of the double-well potential.

3.5 Conclusion

In this chapter, we studied the frequency response of the over-damped double-well potential system with LTspice's AC analysis and numerically evaluated the frequency response of the harmonics of the system. We also suggested another method called the Adomian decomposition method for solving non-linear differential equations with approximation in the time domain, for evaluating the frequency response of the non-linear system, and getting analytical approximations for the dependence between the parameters of the system and the frequency response of the system. Finally inferring from these analyses, the requirements on the system's bandwidth and on the noise's bandwidth for detecting weak signals with some arbitrary frequency were proposed.

Chapter 4

Generating Noise Using Function Generators

In this chapter, to generate the noise signal for input to the hardware implementation of the system, the built-in noise generator mode and the arbitrary waveform generation(AFG) capability of the AFG1022 Tektronix function generator are used. The built-in noise generator has some limitations but the arbitrary waveform generation capability gives freedom to control the bandwidth of the generated noise which is required from the inferences of the previous chapter.

4.1 Built-in Noise Generator

s

The built-in noise generation mode gives control over the peak-to-peak voltage which controls the variance but has a fixed bandwidth for the generated noise signal. The FFT of the generated noise signal is given in figure 4.1.

The FFT is flat till 37 MHz with a magnitude of approximately -30 dB. Changing the peak-to-peak voltage of the function generator increases FFT magnitude up to approximately -10 dB. Since the over-damped double-well potential system has a low-pass

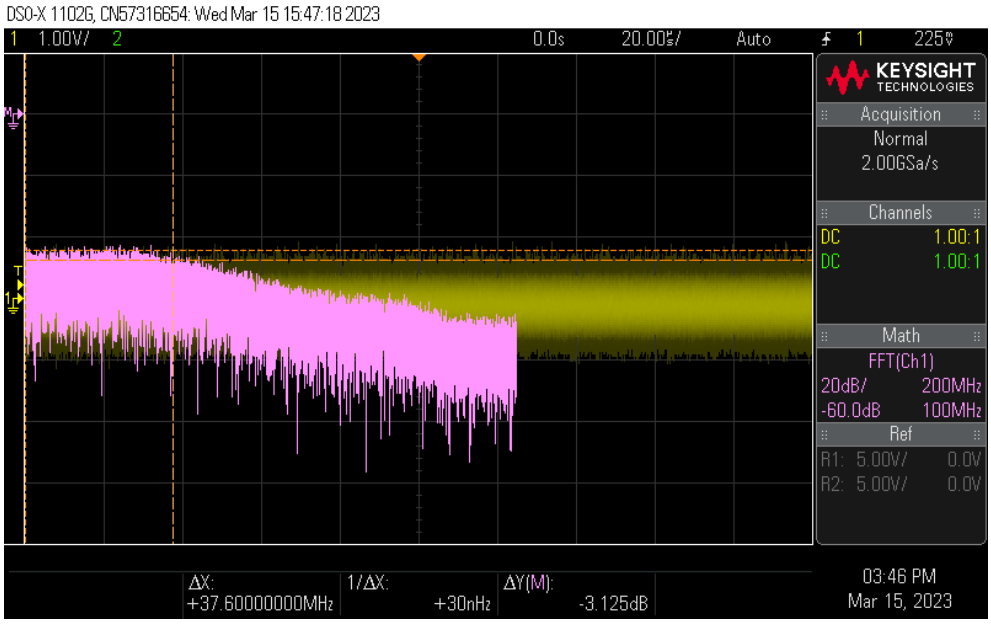

Fig. 4.1: Noise output of the built-in noise generator of AFG1022 (in Yellow) and it's FFT(in Pink)

response, the noise waveform of 37 MHz bandwidth gets filtered to have the bandwidth of the system which is approximately 1.5 kHz. As a result, the total power, which is also the same as the variance of the noise, delivered by the noise waveform within the bandwidth of the over-damped double-well potential system is very low. A simple first-order low-pass filtering of the noise waveform using the RC circuit before giving it as input to this system also did not reflect any changes in the output of the system. Hence this method of generating noise is not used for the experiments.

4.2 Generating Noise Using Arbitrary Waveform Generation Mode

The Tektronix function generators AFG1022 and AFG1062 come with the arbitrary waveform generation(AFG) capability which takes time-value data and produces the waveform as a piece-wise step function. The variance and the bandwidth of the noise waveform produced can be controlled using the AFG functionality. Initially, a noise waveform of

16 kHz sampling rate is uploaded to the AFG1022 function generator. The AFG's noise output is a piece-wise step function of the arbitrary data, hence the frequency response is a sinc function with a 3 dB bandwidth of approximately 3.3 kHz found experimentally. This bandwidth needs to be found numerically in simulations or experimentally and it cannot be solved analytically. The noise generated by the AFG is given as input to the hardware implementation of the over-damped double-well potential system and the outputs are shown in the figures 4.2a, 4.2b and 4.2c, where the bandwidth of the AFG's output is upscaled by the frequency set in the function generator by a factor of 10 successively.

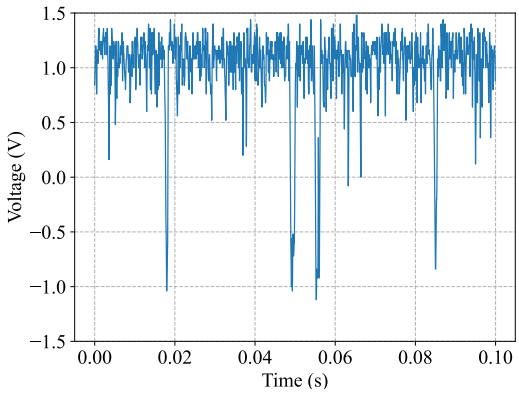

(a) original bandwidth

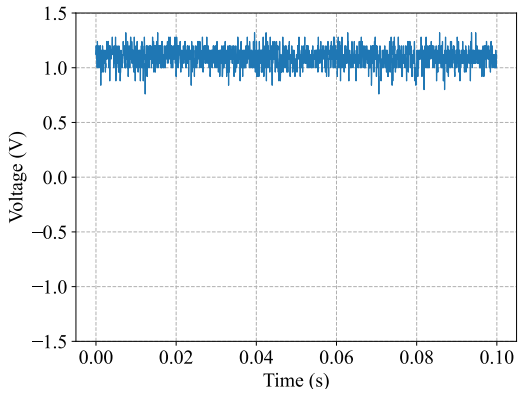

(b) 10*original bandwidth

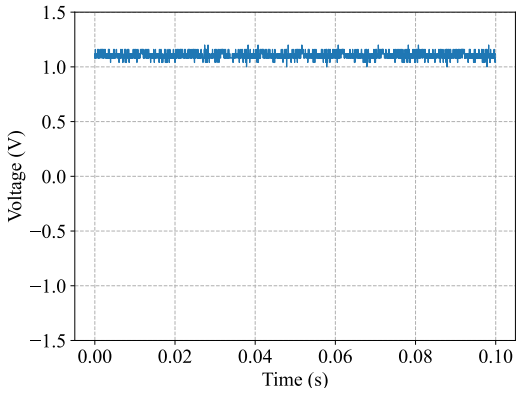

(c) 100*original bandwidth

Fig. 4.2: Noise with a peak-to-peak voltage of 5 V is applied with increasing bandwidths to the hardware implementation of the system resulting in attenuation of the variance at the output

4.3 Conclusion

In this chapter, generating noise waveform for the input to the over-damped double-well potential system using the built-in noise generator and using the arbitrary waveform generation capability of the Tektronix AFG1022 and AFG10622 function generators were discussed. The built-in noise generation functionality has bandwidth limitations, hence it cannot be used. The arbitrary waveform generation capability gives control over the bandwidth and noise variance and hence it is used for generating noise.

Chapter 5

Automation of the Testing Setup

In this chapter, we discuss the details of automating the testing setup with function generators and oscilloscopes with MATLAB using VISA API. We also discuss the practical considerations with which the noise needs to be generated with the function generator.

5.1 VISA API for Test and Measurement Devices

VISA is an acronym for Virtual Instrument Software Architecture. VISA is a Test and Measurement industry-standard communication API (Application Programming Interface) for use with test and measurement devices. Using VISA libraries enables communication for many interfaces such as GPIB, USB, and Ethernet[9]. There are several implementations of VISA API by companies such as Tektronix, Keysight, and National Instruments. The Keysight's IO Library Suite[10] is used in this project for the VISA API. The VISA API can be used by programming in C or MATLAB directly using IVI drivers[11] or by using SCPI commands.

The Standard Commands for Programmable Instrumentation (SCPI) Consortium developed a common interface language between computers and test instruments. The SCPI Standard is built on the foundation of IEEE-488.2, Standard Codes, and Formats. SCPI syntax is ASCII text and can be attached to any computer test language, such as BASIC,

C, or C++. It can also be used with Test Application Environments such as LabVIEW and MATLAB. SCPI is hardware-independent. SCPI strings can be sent over any instrument interface. It works equally well over multiple interfaces such as GPIB, RS-232, VXIbus, or LAN networks[12][13].

5.2 Automating Function Generators

The Tektronix AFG1022/AFG1062 function generators have the capability to generate arbitrary waveforms. It is used to generate noise for the input to the over-damped double-well potential system's circuit model. There are two ways to generate arbitrary waveforms with AFG1022 and they are described in the following subsections.

5.2.1 Tektronix ArbExpress Application

The first method is to use Tektronix software called ArbExpress[14]. The arbitrary waveform data that is to be generated needs to be saved in a text file as a time-value pair which is generated with Python in this project. This needs to be imported to the ArbExpress application. While importing, the time data is discarded and only the value data is considered with their indices. The imported waveform needs to be saved in the "$.tfw$" format. This can be transferred to the pen drive and loaded onto the function generator which will produce the arbitrary waveform. There is an important point to note in this process. Since the ArbExpress application discards the time information while importing the arbitrary data, in the function generator there is an option to set the time period or equivalently the frequency for the arbitrary waveform. The whole arbitrary data will be generated as a waveform within this specified time period and repeated continuously. Consequently, the arbitrary data's bandwidth will be upscaled by the frequency set in the function generator. For example, arbitrary data of a sinusoid of frequency 10 Hz when imported and loaded onto the function generator with the frequency set as 1 kHz in the function generator will produce a sinusoid of 10 kHz.

5.2.2 Programming the Function Generator With MATLAB

The second method is to program the function generator through the VISA API. The function generators have a programmer manual that lists and describes all the SCPI commands that can be used to control all the parameters of a function generator. The AFG1022 programmer manual[15] is referred for the SCPI commands. Along with Tektronix's VISA implementation, basic C and MATLAB program examples for using the VISA API were provided in a directory immediately above the installation directory. The C examples used the IVI drivers while the MATLAB example used the SCPI commands hence MATLAB was chosen to automate the function generator.

The arbitrary data is transferred to the function generator using SCPI commands as a binary block data where several bytes of data are sent as a string of characters with each character corresponding to a byte of data. Each data point of the arbitrary waveform data is represented as an 8-bit integer. The arbitrary waveform is normalized to the maximum absolute magnitude of one before converting to an 8-bit integer representation. This 8-bit data needs to be converted to the corresponding ASCII character which is then used in the binary block data string. From observations, it was found that the arbitrary data's values from -1 to +1 are encoded to a range of 0-67 in decimal values whose ASCII characters are used in binary block data. The programmer manual for AFG1022 indicates that the range of data points that can be uploaded to the edit memory ranges from 2-8192 points. But from observations, it was found that it was possible to upload twice the maximum number of points i.e., 2*8192 = 16384 to the edit memory. It was observed that the firmware of AFG1022 needs to be newer than v1.2.0 for the arbitrary waveform generation functionality to work properly. It had a bug where sweeping from -1V to +1V was working but when sweeping from +1V to -1V the function generator froze and did not produce the outputs.

White Gaussian noise is generated in MATLAB with mean 0 and variance 1 by generating samples from a normal distribution. Each block of data uploaded to the function generator is produced within the time period which is also set using an SCPI command.

The number of data points in the block and the time period set determines the bandwidth of the noise generated. The number of data points to be uploaded in each block is arbitrarily chosen to be 16,000. Now the bandwidth of the noise can be controlled by the time period. Since this noise data will be repeated continuously for every time period length of time, the generated noise may not be truly random. So, a new noise data block is generated and uploaded to the edit memory within each time period. The arbitrary waveform generator's output reflects the contents of the edit memory only after executing an SCPI command setting the output to the contents of the edit memory before which the output continues to generate the previously uploaded data in the edit memory even though the edit memory was uploaded with a different data block. This observation is used to perfectly time the generation of newer noise data exactly at the end of the generation of the previous data.

In this process, the noise data is normalized by dividing by an arbitrarily chosen value of 5, which was greater than the magnitude of the noise samples observed, before uploading to the function generator instead of normalizing each data block with the maximum value observed in that block. Let σ_i^2 be the noise variance and a_i be the maximum magnitude of the noise data of the i^{th} block. When normalizing by the maximum value in each block, the noise variance of the whole sequence σ^2 is given by,

$$\sigma^2 = \frac{1}{N} \sum_{i=0}^{N} \frac{\sigma_i^2}{a_i^2} \tag{5.1}$$

When normalizing by an arbitrarily high value compared to the maximum absolute value in the block of noise data, the variance of the whole sequence of data σ^2 is given by,

$$\sigma^2 = \frac{1}{N} \sum_{i=0}^{N} \frac{\sigma_i^2}{5_i^2} \tag{5.2}$$

Here σ_i^2 is a constant but not a_i. Hence the equation 5.1 is followed for normalizing so that the variance of each data block is the same as that of the whole sequence of data with multiple blocks concatenated.

5.3 Automating Oscilloscope

The Tektronix TDS2014C oscilloscope is used for data acquisition. Data acquired by the oscilloscope can be directly read to MATLAB using VISA API. Along with Tektronix's VISA implementation basic C and MATLAB program example for reading data from oscilloscope was given in a directory immediately above the installation directory. This example program was modified and used to read the oscilloscope data. The MATLAB examples use SCPI commands which are given in the Tektronix TDS200 series programmer manual[16]. There are several parameters in the oscilloscope that need to be set to a known value through an SCPI command for each. The acquire mode should be set to sample and to stop acquiring samples after a sequence. The oscilloscope will stop acquiring data after one instance of acquiring 2500 points covering the full time scale in the oscilloscope. The channel parameters such as coupling, horizontal position, probe scaling, vertical scaling, and horizontal scaling need to be set. The vertical scaling and the vertical offset need to be read from the oscilloscope because the data read from the oscilloscope will be normalized to a maximum magnitude of one and offset as zero. The data encoding format needs to be set to a signed integer with the most significant byte transferred first. The data source needs to be set to the channel from which data needs to be read. The trigger parameters are set to trigger the data acquisition from the particular channel and to trigger for a rising edge. The trigger mode is set to 'normal'. To initiate the data acquisition, the acquire state needs to be set to 'on'. Once the oscilloscope completes acquiring one sequence of data, it generates an operation complete when queried with *OPC? command. Only after the operation complete message is received, the data should be queried to be read from the oscilloscope. The data received will be in binary block data format which is then converted to decimal format using an instrumentation control toolbox function called 'binblockread'. The data is then scaled by the vertical scaling and the vertical offset is added which gives the data that can be used for further processing.

5.4 Conclusion

In this chapter, the details of using VISA API to automate the function generators and the oscilloscope to generate arbitrary data and acquire data were discussed. Automating this testing setup will accelerate the testing process which will help conduct experiment and process the data faster and removes the hassle of using a USB flash drive for testing and data acquisition.

Chapter 6

Stochastic Resonance for Weak Signal Detection

In this chapter, we discuss the practical model of the system with the voltage offsets and present the measurements of the voltage offsets and the threshold voltages of the system. With the inferences from the previous chapters, we try to observe noise-induced switching and stochastic resonance in the hardware implementation of the over-damped double-well potential system.

6.1 Practical System Model With Voltage Offsets

The op-amps and multiplier ICs used in the hardware implementation have some voltage offsets at the inputs which will be reflected in the outputs. The offsets are modeled as voltage sources at the inverting input of the op-amp and one of the inputs for the multiplier IC. The differential equation modeling the hardware implementation is a modification equation 6.1 with the offsets given by,

$$\frac{\mathrm{d}V_2}{\mathrm{d}t} = -\frac{1}{RC_1}\Big(-V_2+((V_2+V_{osm})^2-11V_{oso})(V_2+V_{osm})+9V_{oso}-10V_{osm}+f(t)+Acos(\omega t)\Big) \tag{6.1}$$

where V_{osm} is the offset of the multiplier and V_{oso} is the offset of the op amp.

6.1.1 Measurement of Offset Voltages and Thresholds of the System

The input offset voltages measured for ua741 op amp are in table 6.1. The MPY634 multiplier IC does not have noticeable offsets. The voltage offsets given in table 6.1 are quite small to affect the outputs considerably according to the circuit model with the offsets considered as given in equation 6.1. The ua741 ICs are replaced with op07 ICs and are used to obtain all the outputs in this chapter. op07 op amps have input voltage offsets in the range of a few microvolts. Hence their offsets were not measured.

Name of Opamp	Offset voltage
output_opamp	280 μV
pot_fn_deriv_opamp	-1.16 mV
inverting_amplifier	520 μV

Table 6.1: Op amp input voltage Offsets (The names of the op-amps are as in the schematic diagram of the circuit in KiCAD)

The threshold voltage is defined as the input required to deterministically switch the output to the other minima of the double-well potential in the absence of noise. The threshold voltage measurements are having considerable differences indicating the presence of a strong DC bias compared to the op-amp offsets.

Switching direction	Threshold voltage
+1V to -1V	547 mV
-1V to +1V	-240 mV

Table 6.2: Threshold voltages to switch to the other minima in the double-well potential where the minima are +1V and -1V without any bias

This DC bias is also reflected in the minimum values of the outputs. The minima are

located at +1.08 V and -0.9 V obtained from figure 6.1. By trial and error it was found that when a DC bias of 160 mV is applied to the input, the output minima are located at ±1V. The origin of this DC bias needs to be studied for eliminating it.

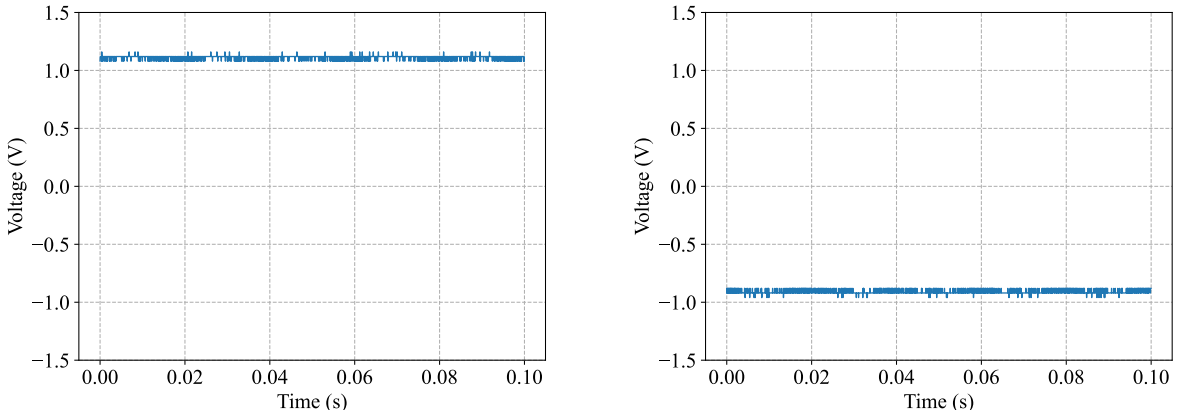

(a) Positive minima

(b) Negative minima

Fig. 6.1: The minima observed from the experimental outputs of the hardware implementation

6.2 Noise Induced Switching

The arbitrary noise generated from AFG1022 with a peak-to-peak voltage of 3 Vpp, a DC bias of 160 mV, and approximately 3 dB bandwidth of 3.3 kHz is given as input to the hardware implementation and the output is given in figure 6.2a along with the FFT of the noise in figure 6.2b.

6.3 Stochastic Resonance

With all the inferences of the previous discussions, in this section, we try to observe stochastic resonance in the hardware implementation of the circuit model of the over-damped double-well potential system. Noise with bandwidth less than this system's bandwidth and with increasing variance by increasing the peak-to-peak voltage of the noise through 2 Vpp, 3 Vpp, 5 Vpp, and 8 Vpp are applied to the system as an input. A subthreshold sinusoid

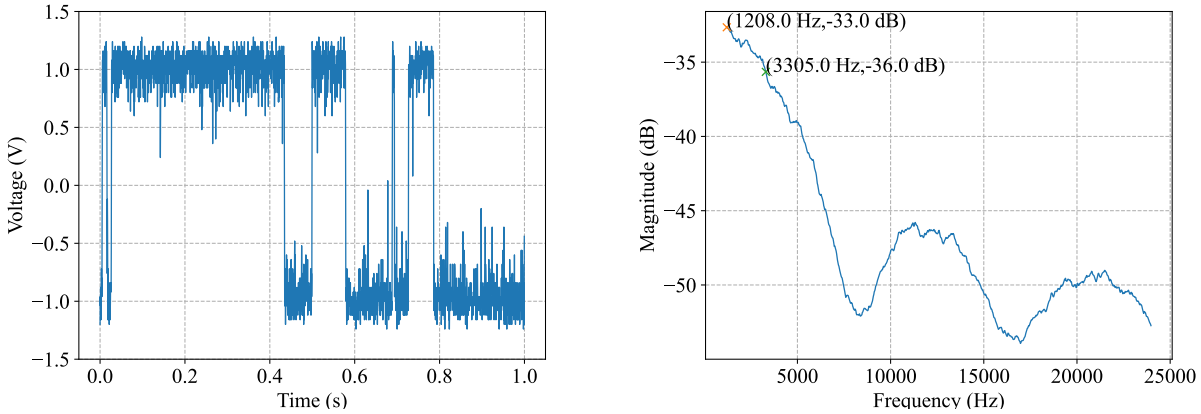

(a) Noise induced switching (b) FFT of noise applied

Fig. 6.2: Experimental noise-induced switching

signal of 100 Hz frequency is applied as another input to the system in all the cases of different noise peak-to-peak voltages. The output voltage of the system and the FFT of the corresponding output are given in the figures 6.3,6.4,6.5 and 6.6. The Signal-to-Noise Ratio (SNR) is measured as the ratio of the energy of the 100 Hz signal to the energy of the noise over the whole bandwidth. The SNR of the outputs measured in each case of noise variance are mentioned in the figures 6.3b, 6.4b, 6.5b and 6.6b. The SNR values observed for increasing noise variance are -23 dB, -17 dB, -10 dB, and -13 dB. It is observed that the SNR increases when noise is increased from 2 Vpp to 5 Vpp and decreases on further increasing the noise to 8 Vpp. This is the characteristic of stochastic resonance observed in a system where the SNR reaches a maximum on increasing the variance of noise before decreasing on further increasing the noise variance.

6.4 Conclusion

In this chapter, the practical model for the circuit implementation of the over-damped double-well potential was discussed. The voltage offset and threshold voltage measurements were presented and these offsets are very small to affect the output. But there is a considerably high DC bias at the output which needs to be eliminated.

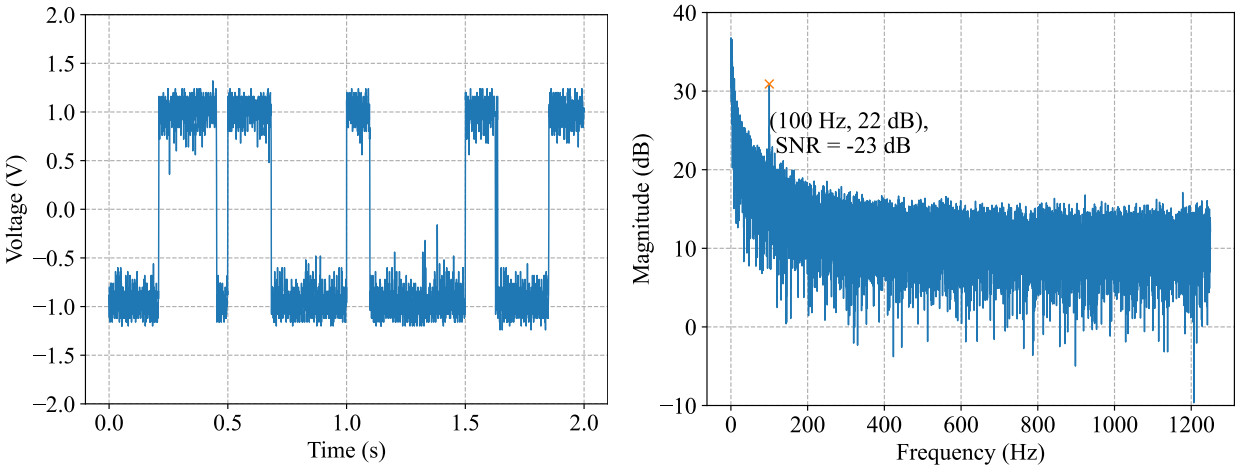

(a) Output (b) FFT of output

Fig. 6.3: Outputs for subthreshold sinusoid of 100 Hz and 2 Vpp noise applied in hardware implementation of the circuit model

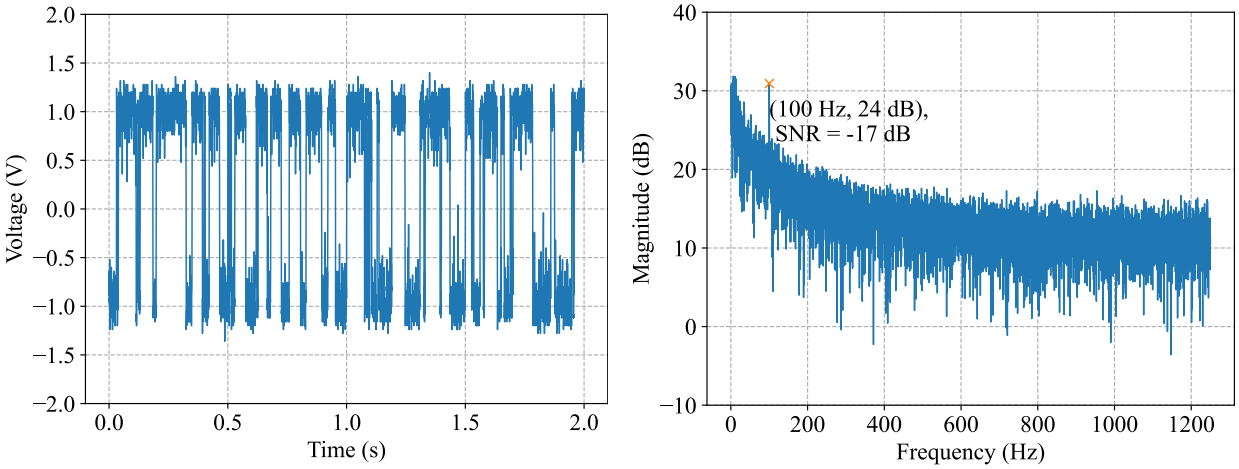

(a) Output (b) FFT of output

Fig. 6.4: Outputs for subthreshold sinusoid of 100 Hz and 3 Vpp noise applied to hardware implementation of the circuit model

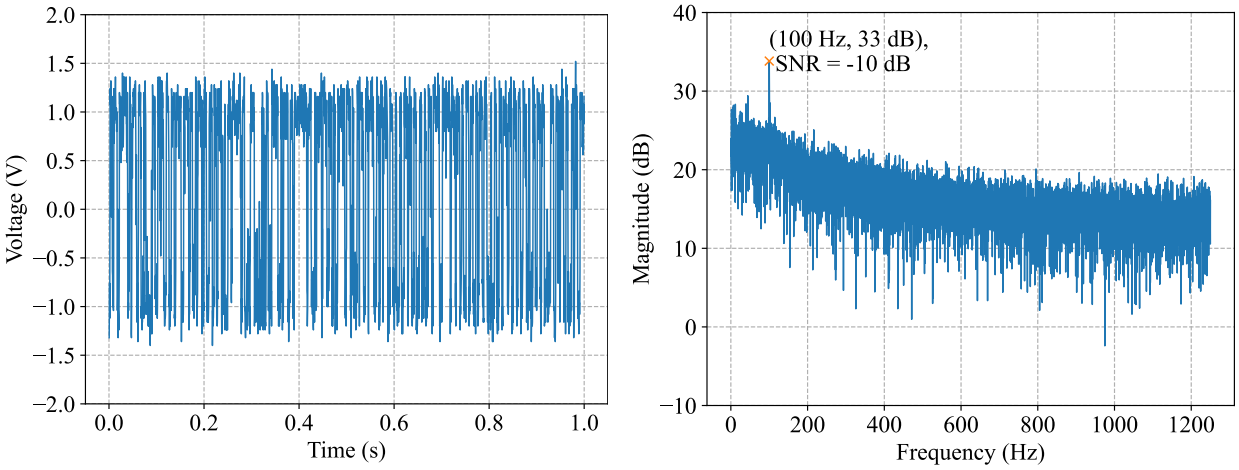

(a) Output (b) FFT of output

Fig. 6.5: Outputs for subthreshold sinusoid of 100 Hz and 5 Vpp noise applied to hardware implementation of the circuit model

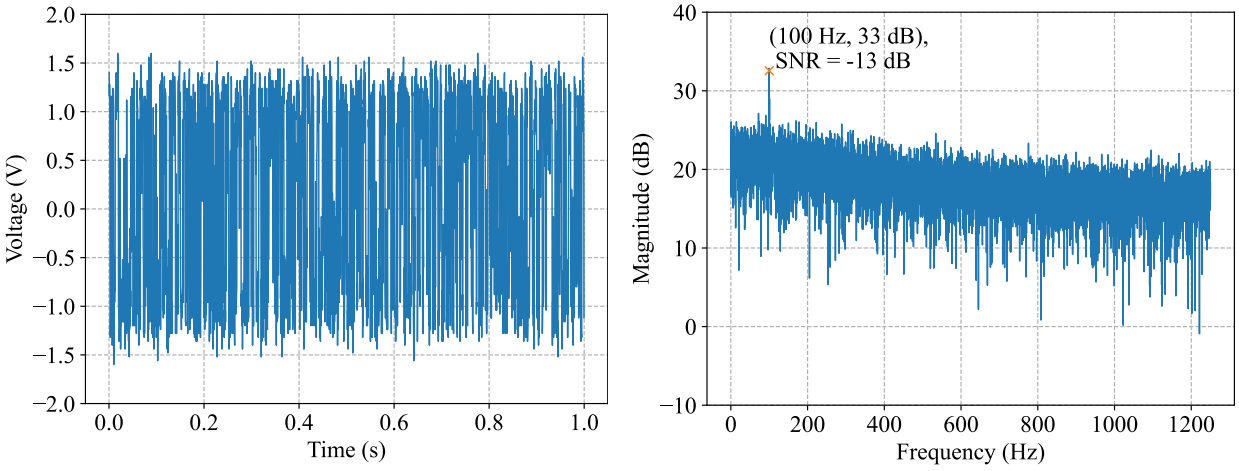

(a) Output (b) FFT of output

Fig. 6.6: Outputs for subthreshold sinusoid of 100 Hz and 8 Vpp noise applied to hardware implementation of the circuit model

Chapter 7

Conclusion and Future Work

The inferences from the frequency response analysis in Chapter 3 provide the necessary constraints on the noise and the input signal's frequency. The experimental observations from Chapter 4 give a direction in choosing the method to generate noise for the experiments. Instructions on automating the function generators and oscilloscopes are discussed in Chapter 5. The experimental results in Chapter 6 display stochastic switching and indicate the observation of the phenomenon of stochastic resonance with the weak signal applied. This indicates that the inferences from the discussions in the previous chapters are right.

As a part of future work, this experimental observation of stochastic resonance in the over-damped double-well potential system needs to be studied systematically and verified. The Kramers time statistics need to be verified. The offsets in the system which are not explained in these discussions need to be studied.

References

[1] B. McNamara and K. Wiesenfeld, "Theory of stochastic resonance," *Physical review A*, vol. 39, no. 9, p. 4854, 1989.

[2] R. Metzler and J. Klafter, "Kramers' escape problem with anomalous kinetics: non-exponential decay of the survival probability," *Chemical Physics Letters*, vol. 321, no. 3-4, pp. 238–242, 2000.

[3] D. G. Luchinsky, R. Mannella, P. V. McClintock, and N. G. Stocks, "Stochastic resonance in electrical circuits. i. conventional stochastic resonance," *IEEE Transactions on Circuits and Systems II: Analog and Digital Signal Processing*, vol. 46, no. 9, pp. 1205–1214, 1999.

[4] M. Ramesh, A. Verma, and A. Ajoy, "Kramers' escape problem for white noise driven switching in ferroelectrics," 2021. [Online]. Available: https://arxiv.org/abs/2112.01373

[5] H. Mulaosmanovic, T. Mikolajick, and S. Slesazeck, "Random number generation based on ferroelectric switching," *IEEE Electron Device Letters*, vol. 39, no. 1, pp. 135–138, 2017.

[6] F. Duan and D. Abbott, "Signal detection for frequency-shift keying via short-time stochastic resonance," *Physics Letters A*, vol. 344, no. 6, pp. 401–410, 2005.

[7] P. Nuij, O. Bosgra, and M. Steinbuch, "Higher-order sinusoidal input describing functions for the analysis of non-linear systems with harmonic responses," *Mechanical Systems and Signal Processing*, vol. 20, no. 8, pp. 1883–1904, 2006.

[8] https://en.wikipedia.org/wiki/Adomian_decomposition_method.

[9] https://www.tek.com/en/support/faqs/what-visa.

[10] https://www.keysight.com/in/en/lib/software-detail/computer-software/io-libraries-suite-downloads-2175637.html.

[11] https://www.ivifoundation.org/resources/default.aspx#:~:text=Short%20IVI%20Getting%20Started%20Guides.

[12] https://www.ivifoundation.org/scpi/default.aspx.

[13] https://en.wikipedia.org/wiki/Standard_Commands_for_Programmable_Instruments#cite_note-4.

[14] https://www.tek.com/en/products/software/arbexpress-signal-generator.

[15] https://www.tek.com/en/arbitrary-function-generator/afg1000-manual-2.

[16] https://www.tek.com/en/oscilloscope/tds210-manual/tds200-series-programmer-manual.